Available online at www.sciencedirect.com
SCIENCE DIRECT®
Remote Sensing of Environment 87 (2003) 482–493
Remote Sensing of Environment
www.elsevier.com/locate/rse

Airborne P-band SAR applied to the aboveground biomass studies in the Brazilian tropical rainforest

João R. Santos*, Corina C. Freitas, Luciana S. Araujo, Luciano V. Dutra, José C. Mura, Fábio F. Gama, Luciana S. Soler, Sidnei J.S. Sant'Anna

National Institute for Space Research-INPE, Av. dos Astronautas, 1758 CP. 515, 12.227-010 São José dos Campos, SP, Brazil

Received 31 August 2001; received in revised form 9 December 2002; accepted 9 December 2002

Abstract

The objective of this study is to evaluate the relationship between the response (σ°) of airborne P-band Synthetic Aperture Radar (SAR) polarimetric data versus biomass values of primary forest and secondary succession. To ensure that different landscapes of "Terra firme" tropical forest of the Brazilian Amazon were represented, a test-site was selected in the lower Tapajós river region (Pará State). The microwave signals from the P-band polarimetric images were related to the aboveground biomass data by statistical regression models (logarithmic and polynomial functions). In the field survey, physiognomic and structural aspects of primary forest and regrowth were collected and afterwards the biomass was estimated using allometric equations based on dendrometric parameters. As an example of the potential use of P-band polarimetric images, they were classified by a contextual classifier (ICM), whose thematic stratification of land use/land cover was associated with biomass class intervals for mapping purposes. The main objective of this P-band experiment is to improve this tool for regional mapping of Amazon landscape changes, due to the growing rate of land use occupation.

Keywords: Tropical rainforest; Biomass; P-band SAR data; Remote sensing; Amazon

1. Introduction

The Brazilian Amazon occupies an area of 5 million km^2 with approximately 76% of this area covered by vegetation types of forest physiognomy. The average gross deforestation rate in the Amazon is approximately 15,700 km^2/year, although this value fluctuates widely due to such factors as the effectiveness of governmental measures in the process of environmental control. More recent data have shown that the conversion of forest areas through deforestation, burning and implantation of agricultural activities, primarily cattle raising, has risen to 604,500 km^2 in this region (INPE, 2002), while 15% of this total amount is estimated to be abandoned land (nonproductive) in a process of natural recovery. Another activity of degradation that is causing concern is timber exploitation. This type of destructive practice has been estimated to occur at a rate of 2500 km^2/year in the *Terra firme* forest areas (Santos, Krug, Araujo, Meira Filho, & Almeida, 2001).

Such activities have been conducted without planning, causing significant environmental damage (fragmentation, loss of biodiversity and soils as well as fertility). The decision-makers on environmental issues use satellite images as an important tool to help inventory and control plans for this huge region. Furthermore, such data sets are also used as a support for the estimation of carbon emission/re-absorption in global climate analysis resulting from large-scale changes of land use/land cover. Frequently a statistical procedure is used to estimate the disturbance area under clouds, which systematically affects some parts of the Amazon region, where multi-temporal data from optical sensor systems are not available. Due to its ability to peer through clouds and sensitivity to aboveground biomass, Synthetic Aperture Radar (SAR) is being used to analyze changes in land use/land cover and biophysical parameters of tropical vegetation types (Saatchi et al., 1999).

In this study, we analyzed X-(HH polarization) and P-band polarimetric SAR data, acquired over a region in Tapajos, using the German *AeroSensing RadarSysteme*. Data were

* Corresponding author. Tel.: +55-12-39456427; fax: +55-12-39456448.
E-mail address: jroberto@ltid.inpe.br (J.R. Santos).

0034-4257/$ - see front matter © 2003 Elsevier Inc. All rights reserved.
doi:10.1016/j.rse.2002.12.001

acquired in September 2000 as part of a cooperative agreement between the Brazilian Army (cartographic mapping) and the National Institute for Space Research-INPE. The objective of the study was to evaluate the capability of P-band data to characterize primary forest and secondary successions and to analyze its relationship to aboveground biomass data. Within this framework, this pioneer experiment in the Brazilian Amazon allows the evaluation of P-band contribution to inventory vegetation through the discrimination of biomass levels in primary forests and secondary succession, and as such contributes to modeling of global changes.

2. Background

Considerable theoretical work supports the potential of SAR as means for estimating aboveground forest biomass. For example, Kasischke, Melack, & Dobson (1997), while describing the use of C-, L- and P-band data for ecological applications, concluded that imaging radars have the capability of monitoring variations in biomass of forested ecosystems, but that this capacity is not consistent for different forest typologies. They found that the upper levels of sensitivity for L- and C-band systems such as SIR-C ranged between <100 ton/ha for complex tropical canopies to ~ 250 ton/ha for simpler forest dominated by a single tree species, but a better performance for biomass estimation was reached using lower frequencies (P- and L-band radar systems with a cross-polarized channel). At these longer wavelengths, microwave scattering and attenuation results from interactions with the tree boles and larger branches found within forests, as well as the ground surface; at these frequencies, the smaller woody stems and the foliage act mainly as attenuators. The dependence of backscatter on aboveground biomass has also been documented by others including: Dobson et al. (1992) and Le Toan, Beaudoin, & Guyon (1992) for pine forest, Rignot, Way, Williams, & Viereck (1994) for boreal forest, Luckman, Baker, Honzak, & Lucas (1998), Santos, Pardi Lacruz, Araujo, & Keil (2002), and Yanasse et al. (1997) for tropical forest. Nevertheless, Kasischke et al. (1997) made a general comment that radar backscatter is correlated not only with total biomass, but also with the different components of biomass, such as branch biomass, needle/leaf biomass, and bole biomass or with other physical tree-stand parameters such as height and basal area.

An estimate of the forest structural dependence of backscatter was provided by Imhoff (1995) who used the Michigan Microwave Canopy Scattering Model and forest canopy biometric data from tropical and subtropical broadleaf forest (including regrowth) to simulate a series of forest stands having equivalent aboveground biomass, but with substantial structural differences. The vegetation surface area to volume ratio (SA/V) was used as a structural descriptor. Based on this theoretical analysis, he reported that structural differences could add a significant amount of error to regression relations below the biomass saturation limit and even lower the saturation level when used to inventory biomass over large areas using SAR. In general, he found an inverse relationship between the SA/V ratio and backscatter, which is positively related to biomass.

Numerous studies using airborne or spaceborne SAR support the potential of SAR for biomass estimation. For example, Imhoff (1995) examined AirSAR biomass data sets for tropical broadleaf evergreen forests in Hawaii and coniferous forests in North America and Europe. The study indicated a saturation level for both types of forests of 20 ton/ha for C-band, 40 ton/ha for L-band and 100 ton/ha for P-band. However, relatively good regression relationships could be derived between radar backscatter and forest biomass taking into account these saturation levels. Luckman, Baker, Kuplich, Yanasse, & Frery (1997) quantified the different sensor responses—ERS-1, JERS-1 and SIR-C—and their dependence on the biomass density of regeneration forest and primary forest. Among the bands analyzed, L_{HV} was found to be the most suitable for biomass estimation with a saturation level of 60 tons/ha. Foody et al. (1997) analyzed SIR-C data in C- and L-bands in the three conventional polarizations (HH, HV and VV) in a region north of Manaus, Brazil. The authors noted a visual discrimination of the main regenerating classes. Although this might indicate a potential to estimate biomass, analysis of the six bands separately produced no significant relationships between SAR backscatter and forest biomass. However, significance improved through the use of an L_{HV}/L_{HH} band ratio and through forest stratification by a dominant species (*Cecropia* sp.) with a C_{VV}/L_{VV} ratio. This shows that band ratios may improve the relationship between backscatter and forest biomass as well as increase the backscatter saturation levels above those described by Imhoff (1995).

A model to estimate forest biomass density was developed by Luckman et al. (1998) in the Brazilian Amazon using JERS-1 data. The authors used field information from the Tapajós and Manaus regions to fit and to validate their model, respectively. Their model was then applied to a mosaic of 90 JERS-1 images and compared with a map derived from NOAA/AVHRR data. The results showed a reasonably good correspondence between the two maps. However, flooded areas were misclassified as nonforested areas in the mosaic, reducing the apparent amount of primary forest. In spite of this, the backscatter saturation levels seemed comparable to other studies of broadleaf forests (Imhoff, 1995).

AirSAR data taken in the Colombian Amazon were used by Hoekman & Quiñones (2000) in order to distinguish different types of land use/cover and estimate biomass. These authors considered four cover types: primary and secondary forest, recently deforested areas and pastures. A maximum likelihood classification was applied to several different combinations of bands and polarizations. After a detailed analysis of all classifications, the L_{HV} and P_{RR}

(circular polarization) combination was chosen. Next, a biomass map was generated based on field information and eight classes that could be identified at a high level of confidence. Although P-band performed best for discriminating between primary forest, secondary forest and pastures, it did not discriminate between forested and recently cut areas well. P-band saturated at a higher level of biomass compared with the aforementioned works (i.e., Imhoff, 1995), covering a biomass range of 10–200 tons/ha that is important for forest secondary regrowth monitoring.

Mapping vegetation using L-, C- and X-band data has limitations (Dobson et al., 1992; Imhoff, 1995; Le Toan et al., 1992; Santos et al., 2002). Radiation at X-band penetrates only the upper section of the tree canopy, and as such radar backscatter (σ°) is only related to the top layer and the crown. C-band penetrates the leaves but not the branches, while L-band encounters leaves and small branches. As a consequence, L band σ° is related to branches and potentially to trunks (FAO, 1993). Compared to the other bands, P-band shows the greatest penetration. In those sections where the crowns and small branches have little influence on the backscatter, P-band backscatter is mainly related to the trunks.

3. Study area

The area selected for this study is located at the lower Tapajós River region (Pará State), limited by geographical coordinates W 54°53′ to 55°06′ and S 3°03′ to 3°12′, close to the village of São Jorge, along highway BR-167 Cuiabá–Santarém. The yearly rainfall varies between 1750 and 2000 mm, with a biological dry period of 40 days, limited by strong downpours. The average yearly temperature is 26 °C. Relative humidity tends to follow the rainfall regime: during February the highest values approach 90%. In this region, distrofic yellow latosols (oxisol) predominate in two textural classes: clay and medium clay. These are normally deep soils, found over hilly to strong hilly terrain, covered by dense forest. According to Projeto RADAMBRASIL (1976), the area under study presents: Dense Ombrophilous Forests of Lowlands with two physiognomies, namely with a large number of emergent individuals or uniform canopy; and there are also sections of Open Forests without palms. Characteristic species include *Carapa guianensis* Aubl., *Eschweilera odorata* (Poepp) Miers, *Syzygiopsis oppositifolia* Ducke, *Trattinickia rhoifolia*, *Tachigalia myrmecophylla* Ducke, *Coumarouma odorata* Aubl., *Nectandra mollis* Nees. Areas of secondary succession are found at different seral stages. They are the result of human agricultural practices and of extensive cattle raising activities, and the most common species are *Tapirira guianensis* Aubl., *Cecropia* spp., *Vismia guianensis* (Aubl) Choisy, *Guatteria poppigiana* Mart., *Didymopanax morototoni* Aubl., *Inga alba* (Sw) Willd. and *Murcia bracteata* (Rich) D.C. Human occupation is related mostly to subsistence agriculture (rice, cassava, maize and beans are the main products), to a few cash crops as pepper and cocoa and to large areas of extensive cattle raising.

4. Materials and methods

4.1. Reference data: descriptions of biophysical parameters

A field campaign was conducted in parallel with the SAR mission to characterize biomass density of primary and second-growth forest. Given a limited time for ground surveys, a compromise was established between the intensity of sampling within a plot and the number of plots acquired. Luckman, Baker, et al. (1997) commented that the intensity of sampling is established by the area of the plot, which determines the potential errors associated with biomass estimated at that site, while the number of samples must be sufficient to cover the required range in biomass density. Thus, both transect sampling and area sampling methods were considered for the field campaign. Based on prior experience (Araujo, Santos, Freitas, & Xaud, 1999; Santos et al., 2002) from studies exploring the association of optical and SAR data as well as data from previous forest inventories from the Amazon, the size of sample plots was limited to 10 × 250m and 10 × 100 m for primary forest and secondary succession, respectively. Each plot was positioned within a homogeneous area of vegetation typology using a GPSII/Garmin system. All plots were buffered from anthropogenic features (roads, pastures, etc.) by a minimum of 50 m for primary forest and 20 m for secondary forest. Within each transect, several parameters were measured, including: diameter at breast height (DBH>5 cm), total height (H), crown cover percentage, and location of each arboreal individual in the plot. In addition, a botanical identification was also performed.

Areas of regeneration were inventoried in order to represent three secondary succession stages, namely: initial (ISS), intermediate (IntSS) and advanced (ASS) stages, in which stratification considered the age of the natural regrowth (defined normally by the temporal evolution with TM-Landsat data) as well as structural and floristic characteristics typical of each seral stage. This resulted in age intervals of below 5 years, from 5 to 15 years, and above 15 years for classes ISS, IntSS and ASS, respectively. Based on the measurements and field analysis, initial stage ‘‘capoeiras’’ (regrowth; ISS) had a mean height of 6 m and DBH of 5.8 cm. Floristic composition was dominated by species such as Vismia *cayennensis* (Jacq.) Pers. (Guttiferae), *Trema micrantha* Blume (Ulmaceae), *Cecropia leucocoma* Miquel. (Moraceae), *Cecropia scyadophylla* Mart. (Moraceae), *Chrysophyllum prieurei* Ducke (Sapotaceae), *Duguetia spixiana* Mart. (Anonaceae) and *Cordia bicolor* A. D.C. (Boraginaceae), which represented 63% of the total of individuals measured out of 64 species identified. Intermediate stage ‘‘capoeiras’’ (IntSS) had an average height of 8 m

Table 1
Geographical coordinates of plots, biomass, number of pixels and P-band backscatter coefficients from primary forest and regrowth areas

Sample	Vegetation type	Coordinate		Biomass (ton ha^{-1})	Size of sample (pixel)	Mean σ° (dB)		
		Latitude	Longitude			HH	HV	VV
1	PF	03°04′ 20.2″	54°54′ 43.3″	271.82	3642	− 7.39	− 4.01	− 6.89
2	PF	03°05′ 11.0″	54°54′ 18.0″	202.69	5394	− 7.70	− 4.21	− 6.98
3	PF	03°05′ 17.5″	54°54′ 54.8″	181.79	711	− 7.80	− 4.47	− 7.81
4	PF	03°05′ 15.2″	54°56′ 56.8″	152.83	2315	− 7.19	− 3.29	− 6.62
5	PF	03°04′ 36.0″	54°55′ 08.0″	231.79	2652	− 7.11	− 4.06	− 6.62
6	PF	03°07′ 26.6″	54°54′ 01.1″	174.76	2293	− 6.14	− 3.57	− 6.67
7	ASS	03°04′ 18.0″	54°55′ 27.5″	111.61	2691	− 6.23	− 4.25	− 6.15
8	ASS	03°06′ 20.4″	54°57′ 50.7″	63.83	1180	− 7.01	− 5.13	− 7.16
9	IntSS	03°04′ 35.4″	54°54′ 05.9″	24.00	558	− 8.16	− 4.80	− 6.27
10	IntSS	03°05′ 59.5″	54°57′ 44.3″	26.95	1130	− 9.31	− 6.38	− 7.86
11	IntSS	03°05′ 58.2″	54°58′ 04.7″	35.52	4238	− 8.97	− 6.57	− 7.72
12	IntSS	03°07′ 55.7″	54°54′ 32.6″	30.48	844	− 6.89	− 4.25	− 6.91
13	IntSS	03°09′ 17.1″	54°56′ 40.4″	22.64	1576	− 7.98	− 4.63	− 7.05
14	IntSS	03°08′ 10.5″	54°54′ 58.2″	26.63	939	− 8.57	− 4.07	− 7.71
15	ISS	03°05′ 11.2″	54°54′ 22.2″	16.05	2214	− 8.84	− 5.58	− 8.14
16	ISS	03°06′ 39.5″	54°55′ 38.8″	5.25	737	− 11.33	− 8.36	− 8.45
17	ISS	03°06′ 39.2″	54°55′ 36.9″	8.27	506	− 10.23	− 7.74	− 8.99
18	ISS	03°10′ 46.4″	54°57′ 09.5″	8.00	1706	− 9.95	− 7.80	− 9.47

PF = primary forest; ASS = advanced; IntSS = intermediate; ISS = initial secondary succession.

and an average DBH of 7.7 cm. Species composition was the same as ISS with the addition of several more species, including *Bagassa guianensis* Aubl. (Moraceae), *Inga falcistipula* Ducke (Leguminosae Mimosoideae) and *V. guianensis* (Aubl.) Choisy. (Guttiferae). These species represented 58% of a total of 121 species with botanical measurements. Advanced "capoeira" (ASS) had an average height of 11 m and average DBH of 11 cm with 105 species identified. *D. spixana* Mart. (Anonaceae), *B. guianensis* Aubl. (Moraceae), *Cariana* sp. (Lecythidaceae), *I. falcistipula* Ducke (Leguminosae Mimosoideae), *V. guianensis* (Aubl.) Choisy. (Guttiferae) and *Cochlospermum orinocense* (H.B.K.) Steud. (Cochlospermaceae) represented 43% of the total trees measured.

During the forest inventory 33 plots were surveyed. Eighteen of these plots were within the area imaged with P-band radar (Table 1). In the partial sampling used in this study, 1571 trees were measured for primary forest and 1639 trees for regenerating areas. The biophysical parameters measured in the forest inventory for each plot permit detailed physiognomic–structural profiles of vegetation cover (Fig. 1). These profiles facilitate the typologic representation and understanding of the images that result from the interaction of radar with vegetation.

Aboveground biomass for primary forest and secondary succession was estimated based on DBH and total height measurements using general allometric equations (Eqs. (1) and (2)), according to Brown, Gillespie, & Lugo (1989) and Uhl, Buschbacher, & Serrão (1988), respectively.

$$\text{biomass} = 0.044 \times (\text{DBH}^2 \times H)^{0.9719} \quad (1)$$

$$\ln \text{biomass} = -2.17 + 1.02\ln(\text{DBH})^2 + 0.39\ln H \quad (2)$$

The use of mathematical models which use variable tree parameters, such as diameter at breast height, trunk height, crown diameter and total tree height, to estimate above-

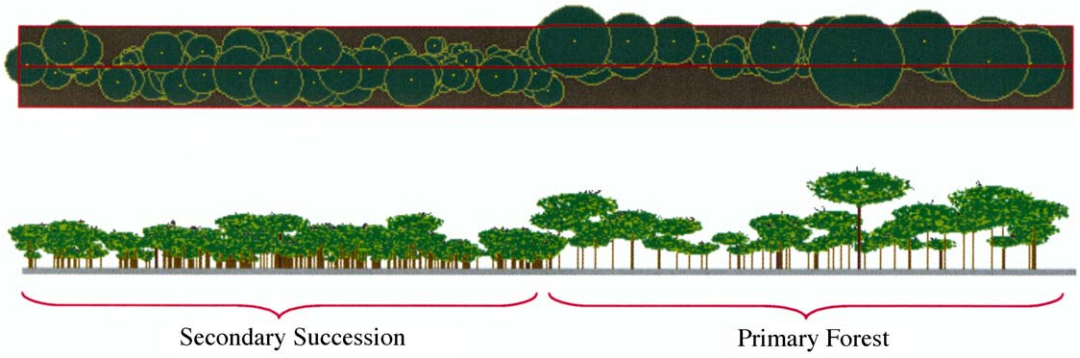

Fig. 1. Physiognomic–structural profile of primary forest and intermediate secondary succession in Tapajós site.

ground biomass indirectly, presents limits to accuracy. According to Brown et al. (1995), there is a lack of consensus as to which is the best estimate for forest biomass in the Brazilian Amazon. There has been a strong debate on this issue by Brown & Lugo (1992) and Fearnside (1992). A comparison between the biomass equations used in previous studies and the establishment of an appropriate mathematical formulation to estimate the vegetation weight of a particular region (Tomé Açu, Pará State) in the Amazon forest was recently conducted by Araújo, Higuchi, & Carvalho (1999). Brown et al. (1995) mention that the main reasons for the wide range of these estimates include: different data sets, different areas or forest types, and different biomass components included in the total biomass values.

In this study, we used the general equation from Brown et al. (1989) to estimate the biomass of primary forest, using as input parameters the DBH and H values. Brown et al. (1995), using this same model, compared it to models that also used the variable S (wood density) and to formulations which only considered DBH in an area of tropical forest in Rondônia State. They found equivalent results, with biomass within 9% of the total biomass estimate. In terms of floristic composition, the most frequently sampled plant families in primary forest, Meliaceae, Bignoniaceae, Moraceae, Violaceae, Sapotaceae, Leguminosae, Lecythidaceae, Rubiaceae, Lauraceae, Burseraceae, Annonaceae, Myristicaceae and Euphorbiaceae, from which we collected dendrometric parameters, are also found in those areas sampled by Brown et al. (1995).

For areas of secondary growth, biomass was estimated using the general equation proposed by Uhl et al. (1988) applied to all seral stages, since species diversity within the sampled areas increased with the age of the regeneration. According to Nelson et al. (1999), who evaluated allometric models in secondary forests from central Amazon, the general equation from Uhl et al. (1988) is adequate for estimating the biomass of trees with a DBH between 7 and 20 cm, but overestimates biomass below this interval. In the case of the Tapajós region, 44% of the trees measured from these regrowth samples occur within this size interval, 50% fall below a DBH of 7 cm and the remaining 6% have a DBH above 20 cm. For mixed-species regressions, a model based only on DBH gives an average deviation between observed and expected DW (total aboveground dry weight) of 19.8%, while adding total height as an additional input variable does not provide much improvement in these mixed-species models (Nelson et al., 1999). It is important to note that the total height of the tree used in the regression models is estimated in the field, and that there is a possibility of error accumulation (systematic and instrumental errors), resulting in a possible underestimate of height, which could affect the performance of the models generated. In the specific case of pasture sections, which were used as complementary information for the P-band thematic mapping, the biomass data were obtained by destructive sampling, drying and weighting the material (three plots of 0.5 m^2 for each of the four sites).

4.2. SAR analysis

The SAR mission was carried out using an airborne polarimetric system, AeS-1 (*AeroSensing Radar Systeme*), providing P-band ($\lambda = 72$ cm) full polarimetric images data, obtained with a middle frequency of 415 MHz, a depression angle of 45° and mean flight altitude of 3216 m. The scenes have a pixel size with 1.5 m range resolution and 0.7 m azimuth resolution, for one look slant range image. These images were obtained from nine flight strips that surveyed the test-sites, with both the same incidence angle and flight direction. The one look slant range images were used to preserve the target's statistical characteristics, and their pixel values were extracted by visual orientation, using field notes and Landsat-TM images as support. Topographic maps and Landsat-TM images were coregistered and used as complementary materials only for the procedure of locating the sample selection sites in the field.

The P-band scenes in both complex and amplitude mode were initially compared to topographic maps, for the orientation of flight strips, in order to visualize different landscapes and to facilitate plotting of points surveyed during the field campaign. Initially, the images were radiometrically corrected according to the antenna pattern using a function based on homogeneous extended areas (primary forest), and afterwards, the polarimetric calibration was done for each polarization (slant range mode), based on the 8 corner reflectors (placed in the field along the flight strips). For the precise positioning of these corner reflectors, differential GPS Pathfinder/Trimble measurements were taken. Initially, the theoretical sigma from each corner reflector was calculated then a correction factor (f) was generated for these corner reflectors according to Eqs. (3) and (4) below.

$$\sigma^\circ \text{ theor.} = \frac{4.\pi}{\lambda^2} \times \text{Effective area/pixel area} \tag{3}$$

$$f = \frac{\sigma^\circ \text{ theor.}}{\text{Amplitude value measured from corner reflector/sen } \theta_{\text{corner}}} \tag{4}$$

The mean correction factor (f_m) based on the arithmetic average of the f values was obtained for each polarization. From this mean correction factor, σ° was obtained at P-band for those points sampled in the field campaign (Eq. (5)).

$$\sigma^\circ = 20\log[f_m \times (\text{measured amplitude of image/pixel})] \tag{5}$$

The response of this airborne SAR data set as well as bio mass data were examined by regression models, using loga rithmic ($y = c\ln x + b$) and polynomial ($y = b + c_1x + c_2x^2 + c_3x^3$) functions.

4.3. Land cover and biomass mapping

The additional mapping of land use/land cover classes was conducted with a classification algorithm specially developed for polarimetric data (Correia, 1998), based on statistical properties of multivariate data by functions derived from the multiplicative model. Three distributions were used for P-band data modeling: the Wishart distribution—homogeneous areas (Lee, Hoppel, Mango, & Miller, 1994), the multivariate K distribution—heterogeneous areas (Lee, Schuler, Lang, & Ranson, 1994) and the G^0 distribution—extremely heterogeneous areas, which is presented in Frery, Müller, Yanasse, & Sant'Anna (1997) for the univariate case. For this thematic stratification, a contextual Markovian classification technique, called Iterated Conditional Modes-ICM (Frery, Yanasse, Vieira, Sant'Anna, & Rennó, 1997), was used, according to the procedure described by Freitas et al. (2001) for the processing of P-band SAR data. The contextual classification begins with a standard maximum likelihood classification map (with equal a priori probabilities) using the same training areas that ICM uses. The ICM algorithm runs until changes from one interaction to another falls below a threshold established by the user; in this case, this threshold was set at 5%. Previous work (Dutra & Huber, 1999; Frery, Yanasse, et al., 1997) has demonstrated that the use of contextual information, at the classification stage, has led to statistically significant improvements in classification, when compared to pixel-based classification with no contextual information. Superiority of any contextual scheme over other contextual ones has not yet been proven. Choice among contextual schemes is a matter of software availability and personal choice.

This thematic classification was simply associated to biomass values allowing mapping of this biophysical parameter of vegetation, particularly for those areas of primary forest and secondary succession. In order to perform this mapping, the input data were multilook complex images as well as P_{HH}, P_{HV} and P_{VV} intensity images.

5. Results and discussion

The results of this work can be evaluated through the qualitative analysis of the P-band SAR images used, the quantitative inspection by graphical representations of the relation among biomass data and σ° values derived from this polarimetric images, and by considering an example of the spatial distribution of biomass at a section of the test-site Tapajós.

5.1. Reference data: descriptions of biophysical parameters

The analysis of dendrometric parameters, such as the DBH and the height and frequency of trees from each transect, can improve the knowledge of the signal response from P-band SAR data. Considering those areas inventoried during the field survey, a representation of the distribution of trees within diameter class (Fig. 2a) and height intervals (Fig. 2b) was prepared with its respective occurrence frequency for both primary forest and second growth. For tree height distribution, three intervals were considered: an upper stratum ($H \geq 20$ m), localized in a euphotic environment, with a discontinuous canopy, ranging mainly between 25 and 30 m; an intermediate stratum (between 10 and 20 m) with a significant distribution of trees in a continuous

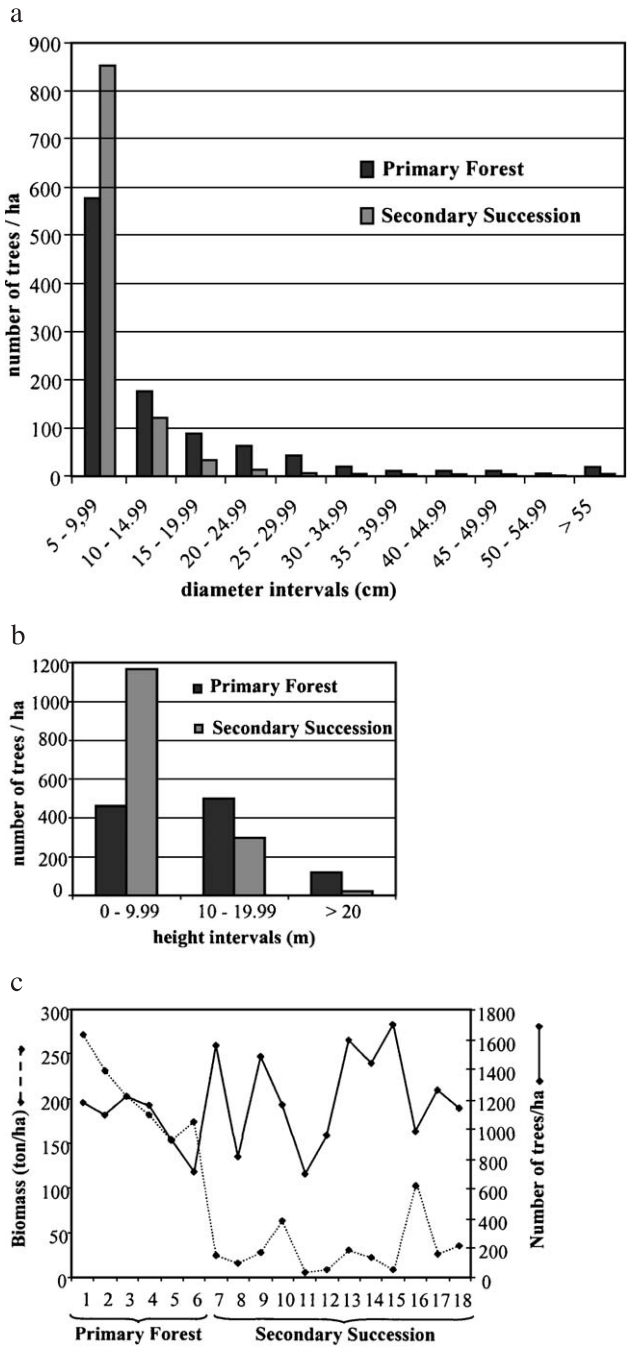

Fig. 2. Diagrams showing the number of trees per class intervals of diameter (a) and height (b) and also versus biomass values (c) of primary forest and regrowth.

understory from 13 to 20 m; and a dense stratum with undergrowth (oligophotic environment), where tree height varied mainly between 6 and 10 m. Secondary succession plots showed a high concentration of individuals in the lower stratum ($H < 10$ m) with a mean biomass of 24.3 tons/ha, an average number of trees estimated at 1400 individuals per hectare (Fig. 2c). Biomass variation within the plots was related to the different stages of regrowth and also to the type and intensity of the land use history, which determines the degree of soil compaction and as a consequence affects the growth of pioneer species. The estimates of biomass for different levels of regrowth at the Tapajós test-site are consistent with other studies (Bernardes, 1998; Salomão, 1994). The high biomass value (111.61 tons/ha) found in the present study (Fig. 2c) for the secondary succession is an indication of more advanced stages of regrowth, as reported also by Salomão (1994), who found values above 80 tons/ha for 20-year-old regrowth. Primary forest plot had a mean biomass of 202.61 tons/ha, with an average of 1035 individuals per hectare (DBH>5 cm).

5.2. Biomass versus σ° data from SAR image

Different types of land use/land cover present their own space of attributes, related to spectral–textural characteristics at P-band images. Fig. 3 presents a small section of the area imaged at Tapajós, showing a scanning line which was used to extract a backscatter (σ°) profile at different polarizations for the different thematic classes. The information contained in this profile corresponds to the characteristics of this series of targets during the dry season, with a monthly (September) rainfall index of 50 mm in this region.

Table 1 shows the number of 1.5×1.4 m pixels (range and azimuth resolution) within each polygon and georectified plot coordinates. Corresponding P-band σ° as well as the respective values of aboveground biomass for those areas of primary forest and secondary succession that were inventoried are also shown.

Based on field survey information related to the biophysical parameters of primary and secondary formations, it is possible to show how P-band backscatter at HH, HV and VV polarizations varies relative to biomass. In order to explore the relationship between these variables, a logarithmic function (Fig. 4) and a third-order polynomial function were used (Fig. 5). Based on this statistical analysis, HH and HV polarizations showed a higher correlation to biomass with higher determination coefficients (r^2) than those of VV polarization. According to these models, 60–70% of the variation in the dependent variable can be explained by the independent variable. Some areas of secondary succession showed similar σ° values as those from primary forest. In these cases, the regrowth typically corresponded to older

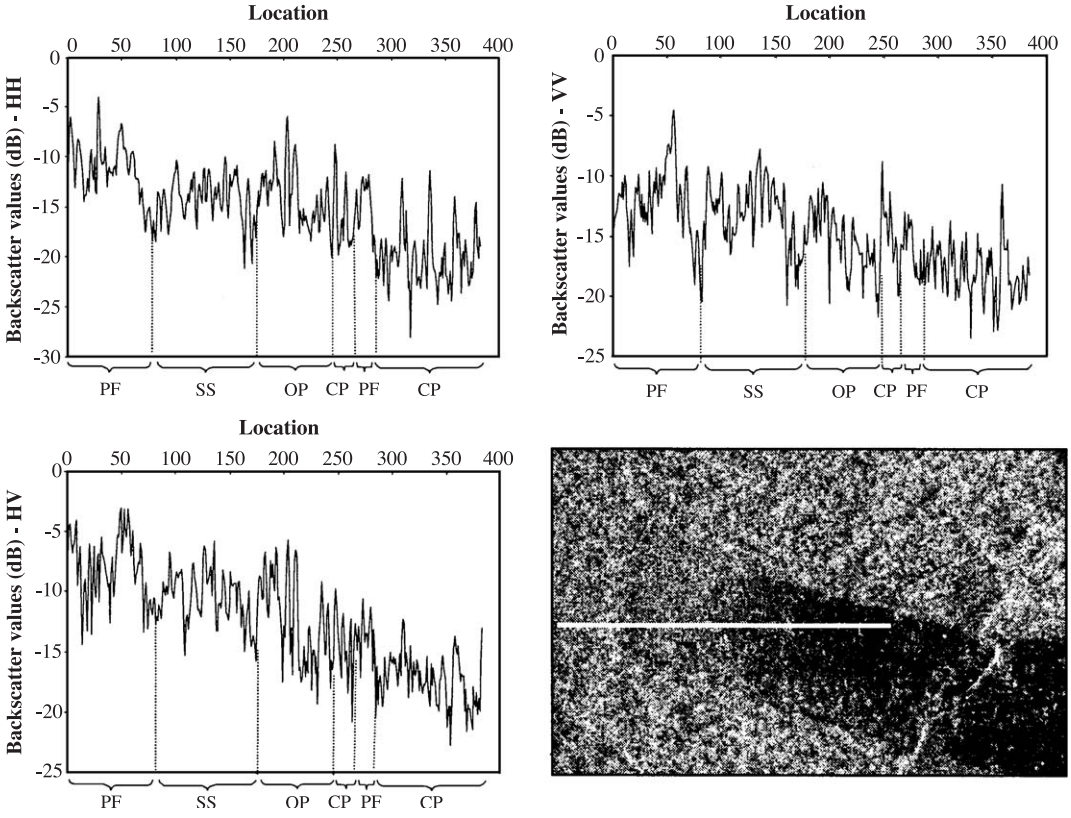

Fig. 3. P-band backscatter from typical land use/land cover classes in Tapajós region, and section of P-band image (HV) (PF = primary forest; SS = secondary succession; OP = overgrown pasture; CP = clean pasture).

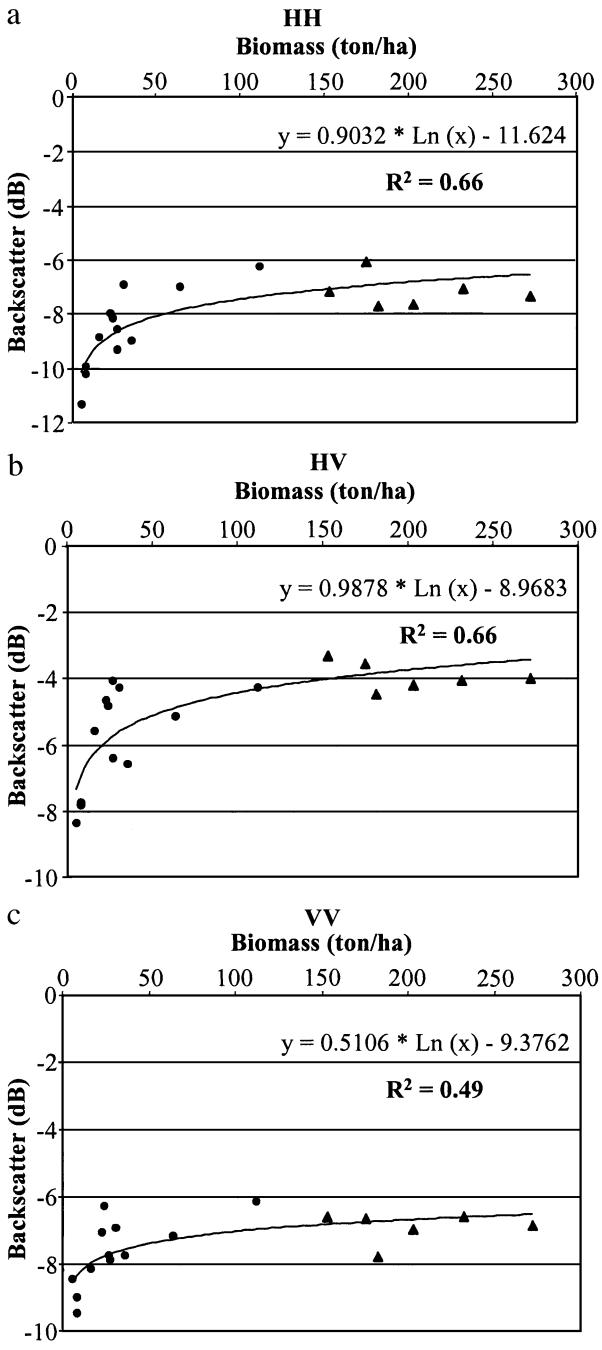

Fig. 4. Backscatter coefficient versus biomass density for all P-band airborne SAR polarimetric images from logarithmic function. (▲ Primary forest; ● Secondary succession).

individuals with a higher number of diameter class intervals and consequently a larger distribution of tree heights. Furthermore, we found no significant difference between models based on HH polarization and those using HV when using a logarithmic function relating biomass to σ° was used (r^2 HH and HV = 0.66). However, although similar r^2 values were found, HV appears to show a better sensitivity because it produced a greater dynamic range. Using a polynomial function, the best fits were produced using the HH polarization ($r^2 = 0.77$). Nevertheless, the model based on the HV polarization showed a dynamic range with greater amplitude. Le Toan et al. (1992), while analyzing SAR data from P-, L- and C-bands at multiple polarizations, noted that the dynamic range of forest backscatter decreased with increasing frequencies and decreased from HV to HH and VV polarization. Despite some differences in the response curves of both models relating backscatter to biomass, the P-band signal saturation appears to be at lower bound than 100 tons/ha, as also reported by Imhoff (1995).

In order to evaluate quantitatively the saturation point with a reasonable statistical confidence, a greater number of

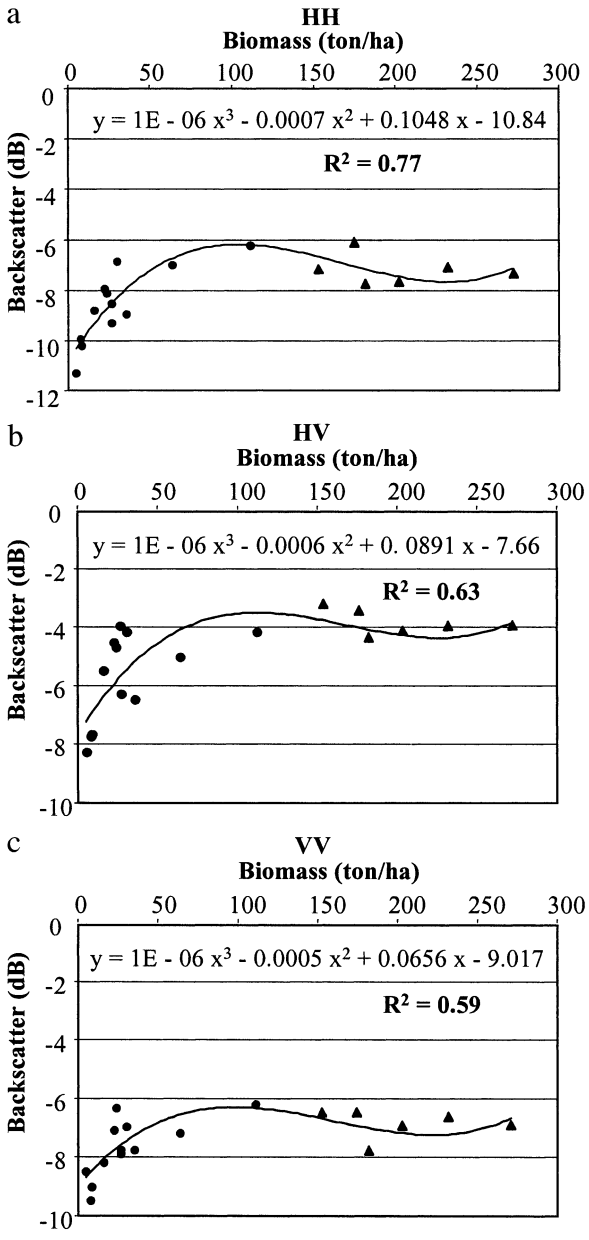

Fig. 5. Backscatter coefficient versus biomass density for all P-band airborne SAR polarimetric images from polynomial function. (▲ Primary forest; ● Secondary succession).

plots should be taken, which will be investigated in near future. It was expected that the cross-polarization would have a higher response than HH polarization, because the signal behavior for broadleaf dense forest is related to how the biomass is partitioned in the imaged area, the structure of branches and twigs, and also the diversity of branching angles in the different types of vegetation cover from this tropical region (Imhoff, 1995). A multiple regression, considering the different polarizations as variables, did not increase the significance of the values of the determination coefficient (r^2), compared to those of simple regressions, when using variables HH or HV separately. According to Kasischke et al. (1997), some theoretical models show the different dependence of backscatter on the overall structure of vegetation canopies with some dependence on variability in the characteristics of the ground layer. Santos et al. (2003) described some preliminary results in this area, aiming to understand the influence of some structural variables (intervals of tree diameter and height, basal area) and, also, the floristic aspects (diversity index) on the P-band response of the primary and secondary forest in this section of the Tapajós region. Another important factor to consider in terms of microwave interactions is related to polarization, in which co-polarizations are more sensitive to canopy structural arrangements (Imhoff, 1995).

An important factor to consider in the analysis of the relationship between backscatter and biomass involves the potential impact of a change in incidence angle over the sample plots. According to our calculations of the nine tracks that covered the study region, we determined that all plots were located at an average incidence angle of 31.9° ($\sigma = 1.17°$) in relation to the image generated. Through the analysis of this small standard deviation, we were able to verify that there was no significant variation in incidence angle between the plots, which would result in a certain angular dependence of backscatter related to biomass data.

All the results described were derived from relatively few plots, each one showing intra-class variations in terms of biomass. Therefore, they must be interpreted cautiously if one wishes to expand these models to other areas of the Amazon. However, based on our experience from the data analysis in the Tapajós region, it is evident that P-band images are suitable for discriminating between areas of primary and secondary forest, separating different stages of natural vegetation growth as well as separating undisturbed primary forest from disturbed forest (e.g. timber exploitation activities).

5.3. Land cover and biomass mapping

At this point, we would like to evaluate the capability of polarimetric P-band data for characterizing and mapping thematic land use/land cover classes in association with biomass values, especially for primary forest and second growth. Using the statistical properties of multivariate data with functions derived from the multiplicative model, Freitas et al. (2001) used P-band SAR data to identify eight classes: primary forest, very old regrowth, old regrowth, intermediate regrowth, new regrowth, bare soil, crop/pasture and floodplain areas, with an estimated *Kappa* classification coefficient of 0.564. Using the same methodological approach, but combining and renaming classes, we derived six thematic classes, namely: primary forest (PF); advanced (ASS), intermediate (IntSS) and initial (ISS) secondary succession; crop/pasture (CP), floodplain areas (F). Using the contextual ICM classification technique to map these six thematic classes, we produced a *Kappa* coefficient of 0.834 with an overall accuracy of 89%. In this process of accuracy assessment, there is an auto-correlation effect of backscatter among pixels. Nevertheless, in this case such auto-correlation was considerably reduced due to the fact we are using a multilook image, formed by averaging 2×5 pixels (range versus azimuth). Training and test samples were based on reference data in the field during the P-band campaign and on a prior knowledge of other studies in this area (Angelis, Freitas, Valeriano, & Dutra, 2002; Luckman, Baker, et al., 1997; Luckman, Frery, Yanasse, & Groom, 1997; Yanasse et al., 1997). All land-use classes were classified by the ICM algorithm, except the floodplain class which was extracted by a threshold procedure because this class showed very high digital numbers related to the other classes. So the floodplain class lacks training samples only the test samples.

Table 2 shows the error matrix, while Fig. 6 shows the map of land use/land cover for a portion of the study area

Table 2
Error matrix for the ICM classifier on P-band data at the Tapajós test-site

		Ground truth						Size of sample (pixels)	
		PF	ASS	IntSS	ISS	CP	F	Training	Test
CLASSIFICATION	PF	56.18	0.84	0.00	15.44	0.23	16.43	13,810	10,287
	ASS	34.03	97.82	26.54	16.45	0.44	0.43	46,936	30,201
	IntSS	1.38	0.95	62.92	53.44	1.50	0.14	3192	2980
	ISS	8.28	0.01	7.58	14.67	0.17	0.00	3418	1179
	CP	0.00	0.37	2.95	0.00	97.66	0.00	32,864	29,965
	F	0.13	0.00	0.00	0.00	0.00	83.00	–	694
	Total	100.00	100.00	100.00	100.00	100.00	100.00	100,220	75,306

PF = primary forest; ASS = advanced secondary succession; IntSS = intermediate secondary succession; ISS = initial secondary succession; CP = crop/pasture; F = floodplain areas.

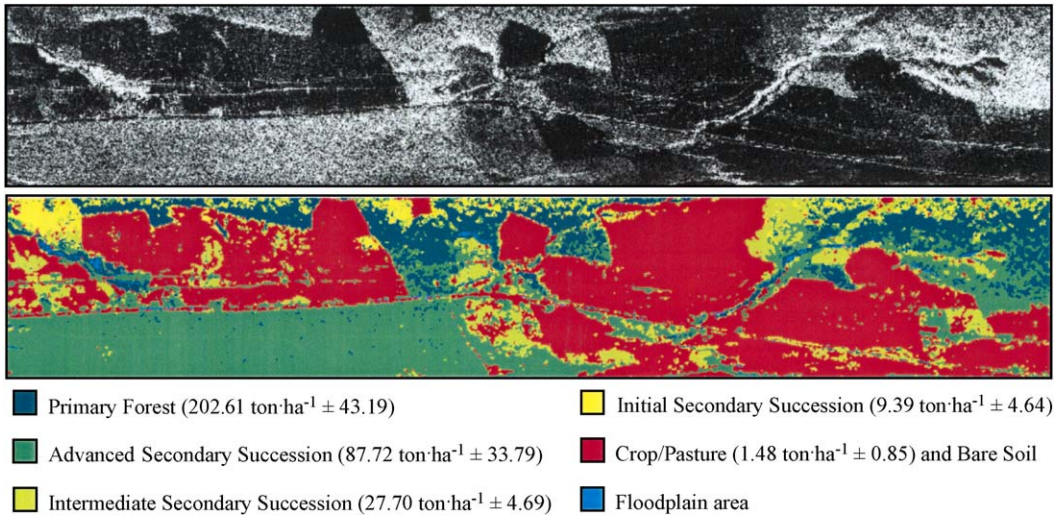

Fig. 6. Sections of P-band image (HV polarization) and map with land use land/cover classes associated with biomass intervals of the primary forest and regrowth stages.

combined with the spatial distribution of biomass for primary forest and second growth. Although the overall accuracy is quite high (89%), it should be viewed with some caution, given some idea of the problems that might occur when a classification with P band is performed. It cannot be extended over the whole area, since the training and test samples were taken based on the available data collected in the field work for each class, and they are not necessarily proportional to the area corresponding to each class over the whole region. The noticeable confusion between ISS and IntSS can be attributed to previous land use, fragmentation type and the diversity of species. The initial stages of succession develop very fast after clearing, leading to higher backscatter than other stages and a tendency to cause confusion in the classification process. It has already been documented that deforestation, when followed by intense land use and abandonment to second growth, leads to lower regeneration rates (Uhl et al., 1988). According to Uhl et al. (1988), biomass may reach 90 tons/ha in 8-year-old regrowth where soils did not suffer intense use; however, in areas with moderate or intense use of soil this rate decreases significantly (35 or 5 ton/ha, respectively). This type of confusion among different stages has been reported by Angelis et al. (2002) where secondary successions between 4 and 8 years old showed different radar backscatter depending on prior land use. Stands which did not experience intense use had radar backscatter comparable to second growth stands much older (9–15 years).

The biomass values associated with each thematic class included in this map (Fig. 6) were produced using the average of biomass data derived from the inventories of primary forest and the different regrowth stages (Table 1). As was previously mentioned in the methodology, the classification procedure was based on polarimetric information, using the appropriate statistical modeling for each class. Using both pattern recognition applied to the images and experience obtained during field survey, it was possible, from the analysis of this classification, to extend biomass values sampled for each class to the entire area under investigation, as well as develop some indication of possible intra-class variation. For example, we found out that the areas of ISS and IntSS were represented in the P_{HH} images by values of -10.09 and -8.31 dB, fluctuating by less than ± 1 dB, while classes ASS and PF had average backscatter values of -6.62 and -7.22 dB, and a variability of approximately ± 0.5 dB, respectively. In the P_{HV} images, areas of secondary succession had average backscatter between -7.37 dB (ISS) and -4.69 dB (ASS), while the primary forest areas had higher backscatter than -3.94 dB. All these classes showed similar dB fluctuations as those found with P_{HH}-band data. These polarimetric responses are pertinent to the conditions of aboveground biomass found in the area under investigation, which are also influenced by the physiognomic–structural characteristics of the vegetation typology from the Tapajós region.

During the classification procedure, we took care that the training samples (also identified and georeferenced in the field) from P-band images were taken at a geographical distance from the test samples, assuming that there is an independence among them. Within the distributions used in this system, derived from a multiplicative model applied to polarimetric data, the G° distribution showed the best fit for all thematic classes, except advanced secondary succession, in which data were best modeled with a K distribution, as mentioned by Freitas et al. (2001).

6. Conclusions

This was the first experience with digital analysis of polarimetric P-band data in the Brazilian Amazon. We found that such data can make a substantial contribution

for the development of models to monitor the dynamics of biomass in tropical rainforest regions, especially in those areas where it is difficult to obtain data from optical sensors. Generally speaking, logarithmic and polynomial functions (third order) had an adequate performance to fit the distribution of biomass versus backscatter data. As expected, HH and HV polarizations possessed higher r^2 than VV polarization. P-band backscatter (σ°) was, in certain cases, similar values between primary and secondary forests, especially in those sequential stages of regrowth, where the structural differences of vegetation cover are not as evident, since they are influenced by local soil conditions, diversity of floristic composition, history and intensity of land occupation and recovery capacity of a certain area.

The ICM classification technique, based on three types of distributions used to model the polarimetric data, is adequate for thematic mapping (*Kappa* = 0.834). Considering even the omission and commission errors between some classes, the thematic mapping, when associated with appropriate biomass values, allows a synoptic analysis of the present inventory of biophysical parameterization of the vegetation cover, which is very important for the regional modeling of the emission and re-absorption of carbon from a certain area and its influence in studies of global change.

In future studies, we expect to process all P-band images from the Tapajós test-site, which will allow the use of all samples inventoried during the field survey, increasing the degree of confidence of the information obtained. This effort will help us define better regression functions that are differentiated for areas of primary forest and for those of secondary succession, including a more refined map of biomass, based specially in the model of best fit among the variables. Taking into account that the P-band data acquired are polarimetric, another important possibility for the analysis is to use biophysical indices, such as the biomass index (BMI), described by Pope, Rey-Benayas, & Paris (1994).

This study is a contribution to the Program of ''Science and Technology for the Management of Ecosystems'' (PPA 2000–2003) from the Brazilian Ministry for Science and Technology-MCT, searching for tools to inventory and monitor environmental issues in the Amazon.

Acknowledgements

The authors acknowledge CNPq (grants 300677/91-0, 380597/99-3 and 300927/92-4) and FAPEMIG (grant #CRA 00054/00) support. The authors wish to thank the 8th BEC (Brazilian Arm), IBAMA/MMA, SUDAM for logistic support, Dr. Edson Sano (CPAC/Embrapa) for providing the aboveground biomass of pasture, Dr. Dar Roberts and the reviewers for the scientific suggestions. This research is a partial result inside LBA LC-11 project, and the scientific cooperation between INPE and DSG (Diretoria do Serviço Geográfico).

References

Angelis, C. F., Freitas, C. C., Valeriano, D. M., & Dutra, L. V. (2002). Multitemporal analysis of land use/land cover JERS-1 backscatter in Brazilian tropical rainforest. *International Journal of Remote Sensing*, *23*(7), 1231–1240.

Araujo, L. S., Santos, J. R., Freitas, C. C., & Xaud, H. A. M. (1999). The use of microwave and optical data for estimating aerial biomass of the savanna and forest formations at Roraima State, Brazil. *Proceedings of the IGARSS'99 Symposium,* Hamburg, Germany [CD-ROM].

Araújo, T. M., Higuchi, N., & Carvalho Jr., J. A. (1999). Comparison of formulae for biomass content determination in a tropical rain forest site in the state of Pará, Brazil. *Forest Ecology and Management*, *117*, 43–52.

Bernardes, S. (1998). Índices de vegetação e valores de proporção na caracterização de floresta tropical primária e estádios sucessionais na área de influência da Floresta Nacional do Tapajós-Estado do Pará. Instituto Nacional de Pesquisas Espaciais-INPE. São José dos Campos, SP, Brasil. Dissertação de Mestrado em Sensoriamento Remoto, 86 pp. (INPE-6890-TDI/651).

Brown, I. F., Martinelli, L. A., Thomas, W. W., Moreira, M. Z., Ferreira, C. A. C., & Victoria, R. A. (1995). Uncertainty in the biomass of Amazonian forests: An example from Rondônia, Brazil. *Forest Ecology and Management*, *75*, 175–189.

Brown, S., Gillespie, A. J. R., & Lugo, A. E. (1989). Biomass estimation methods for tropical forest with applications to forest inventory data. *Forest Science*, *35*(4), 881–902.

Brown, S., & Lugo, A. E. (1992). Aboveground biomass estimates for tropical moist forests of the Brazilian Amazon. *Interciencia*, *17*(1), 8–18.

Correia, A. H. (1998). Projeto, desenvolvimento e avaliação de classificadores estatísticos pontuais e contextuais para imagem SAR polarimétricas. Instituto Nacional de Pesquisas Espaciais-INPE. São José dos Campos, SP., Brasil. Dissertação de Mestrado em Sensoriamento Remoto (INPE 7178-TDI/069).

Dobson, M. C., Ulaby, F. T., Le Toan, T., Beaudoin, A., Kasischke, E. S., & Christensen, N. (1992). Dependence of radar backscatter on coniferous forest biomass. *IEEE Transactions on Geoscience and Remote Sensing*, *30*(2), 412–415.

Dutra, L. V., & Huber, R. (1999). Feature extraction and selection for land use classification from ERS-1/2 InSar data. *International Journal of Remote Sensing*, *20*(5), 993–1016.

FAO—Food and Agriculture Organization (1993). Radar imagery: Theory and interpretation (Lecture notes). Rome, Italy, 103 pp., RSC Series no. 67.

Fearnside, P. M. (1992). Forest biomass in Brazilian Amazônia: Comments on the estimate by Brown and Lugo. *Interciencia*, *17*(1), 19–27.

Foody, G. M., Green, R. M., Lucas, R. M., Curran, P. J., Honzak, M., & Amaral, I. D. (1997). Observations on the relationship between SIR-C radar backscatter and the biomass of regenerating tropical forests. *International Journal of Remote Sensing*, 687–694.

Freitas, C. C., Sant'Anna, S. J. S., Soler, L. S., Santos, J. R., Dutra, L. V., Araujo, L. S., Mura, J. C., & Hernandez Filho, P. (2001). The use of airborne P-band radar data for land use and land cover mapping in Brazilian Amazonia. *Proceedings of the IGARSS'01 Symposium,* Sydney, Australia [CD-ROM].

Frery, A. C., Müller, H. J., Yanasse, C. C. F., & Sant'Anna, S. J. S. (1997). A model for extremely heterogeneous clutter. *IEEE Transactions on Geoscience and Remote Sensing*, *35*, 648–659.

Frery, A. C., Yanasse, C. C. F., Vieira, P. R., Sant'Anna, S. J. S., & Rennó, C. D. (1997). A user-friendly system for synthetic aperture radar image classification based on grayscale distributional properties and context. *Proceedings of the X Brazilian Symposium of Computer Graphic and*

Image Processing (pp. 211–218). Campos de Jordão, Brazil: Computer Brazilian Society.

Hoekman, D. H., & Quiñones, M. J. (2000). Land cover type and biomass classification using AirSAR data for evaluation of monitoring scenarios in the Colombian Amazon. *IEEE Transactions on Geoscience and Remote Sensing*, *38*(2), 685–696.

Imhoff, M. L. (1995). Radar backscatter and biomass saturation: Ramifications for global biomass inventory. *IEEE Transactions on Geoscience and Remote Sensing*, *33*, 511–518.

INPE (2002). *Monitoring of the Brazilian Amazonian forest by satellite 2000–2001*. São José dos Campos, Brazil: National Institute for Space Research-INPE, 23 pp.

Kasischke, E. S., Melack, J. M., & Dobson, M. C. (1997). The use of imaging radars for ecological applications—A review. *Remote Sensing of Environment*, *59*, 141–156.

Lee, J. S., Hoppel, K. W., Mango, S. A., & Miller, A. R. (1994). Intensity and phase statistics of multilook polarimetric and interferometric SAR imagery. *IEEE Transactions on Geoscience and Remote Sensing*, *32*, 1017–1028.

Lee, J. S., Schuler, D. L., Lang, R. H., & Ranson, K. J. (1994). *K* distribution for multilook processed polarimetric SAR imagery. *Surface and Atmospheric Remote Sensing: Technologies, Data Analysis and Interpretation* (pp. 2179–2181). Piscataway: IEEE.

Le Toan, T., Beaudoin, A., & Guyon, D. (1992). Relating forest biomass to SAR data. *IEEE Transactions on Geoscience and Remote Sensing*, *30*(2), 403–411.

Luckman, A., Baker, J., Honzak, M., & Lucas, R. (1998). Tropical forest biomass density estimation using JERS-1 SAR: Seasonal variation, confidence limits, and application to image mosaics. *Remote Sensing of Environment*, *63*, 126–139.

Luckman, A. J., Baker, J., Kuplich, T. M., Yanasse, C. C. F., & Frery, A. C. (1997). A study of the relationship between radar backscatter and regenerating tropical forest biomass for spaceborne SAR instruments. *Remote Sensing of Environment*, *60*, 1–13.

Luckman, A. J., Frery, A. C., Yanasse, C. C. F., & Groom, G. B. (1997). Texture in airborne SAR imagery of tropical forest and its relationship to forest regeneration stage. *International Journal of Remote Sensing*, *18*(6), 1333–1349.

Nelson, B. W., Mesquita, R., Pereira, J. L. G., Souza, S. G. A., Batista, G. T., & Couto, L. B. (1999). Allometric regressions for improved estimate of secondary forest biomass in the central Amazon. *Forest Ecology and Management*, *117*, 149–167.

Pope, K. O., Rey-Benayas, J. M., & Paris, J. F. (1994). Radar remote sensing of forest and wetland ecosystems in the Central American Tropics. *Remote Sensing of Environment*, *48*, 205–219.

Projeto RADAMBRASIL (1976). Folha SA. 21 Santarém; geologia, geomorfologia, solos, vegetação e uso potencial da terra. Rio de Janeiro, 522 pp. (Levantamento de recursos naturais, 10).

Rignot, E., Way, J. B., Williams, C., & Viereck, L. (1994). Radar estimates of aboveground biomass in boreal forests of interior Alaska. *IEEE Transactions on Geoscience and Remote Sensing*, *32*, 1117–1124.

Saatchi, S., Shimard, M., Njoku, E., De Grandi, G., Justice, C., Laporte, N., & Massart, M. (1999). Study of land-use and deforestation in Central and West African Tropical Forest using high resolution SAR satellite imagery. *JERS-1 Science Program'99 PI Reports, Global Forest Monitoring and SAR Interferometry* (pp. 133–138). Japan: NASDA.

Salomão, R. P. (1994). Estimativas de biomassa e avaliação do estoque de carbono da vegetação de florestas primárias e secundárias de diversas idades (capoeiras) na Amazônia Oriental, Município de Peixe-boi, Pará. Universidade Federal do Pará. Dissertação de Mestrado em Ciências Biológicas.

Santos, J. R., Araujo, L. S., Freitas, C. C., Soler, L. S., Gama, F. F., & Dutra, L. V. (2003). Analysis of forest biomass variation in the Amazon and its influence on the response of P-band SAR polarimetric data. In M. Owe, G. D'urso, & L. Toulis (Eds.), *9th International Symposium on Remote Sensing-SPIE, Agia Pelagia, Greece, Sept. 23–27th*. Proceedings of SPIE, Vol. 4879, Remote Sensing for Agriculture, Ecosystem, and Hydrology IV (pp. 252–259). Bellingham, WA: SPIE.

Santos, J. R., Krug, T., Araujo, L. S., Meira Filho, G., & Almeida, C. A. (2001). Dados multitemporais TM/Landsat aplicados ao estudo da dinâmica de exploração madeireira na Amazônia. *Anais do X Simpósio Brasileiro de Sensoriamento Remoto*. Foz do Iguaçu-PR, Brasil [CD-ROM].

Santos, J. R., Pardi Lacruz, M. S., Araujo, L. S., & Keil, M. (2002). Savanna and tropical rainforest biomass estimation and spatialization using JERS-1 data. *International Journal of Remote Sensing*, *23*(7), 1217–1229.

Uhl, C., Buschbacher, R., & Serrão, E. A. S. (1988). Abandonned pastures in eastern Amazonia: I. Patterns of plant sucession. *Journal of Ecology*, *76*, 663–681.

Yanasse, C. C. F., Sant'Anna, S. J. S., Frery, A. C., Rennó, C. D., Soares, J. V., & Luckman, A. J. (1997). Exploratory study of the relationship between tropical forest regeneration stages and SIR-C L and C data. *Remote Sensing of Environment*, *59*(2), 180–190.